

Vol. 791, Series R. 2. 26
103-92

Effect of Coupling Agent on the Dispersion of PETG Montmorillonite Nanocomposite films.

Ajit Ranade, Nandika D'Souza, Bruce Gnade¹, Christopher Thellen², Caitlin Orroth², Danielle Froio², Jeanne Lucciarini², Jo Ann Ratto²

University of North Texas, Denton, Texas 76203-5310

¹University of Texas at Dallas, Dallas, Texas 75083-0688

²U.S. Army Soldier System Command, Kansas Street, Natick, MA 01760-5020

Abstract

Polyethylene terephthalate glycol (PETG) is a clear amorphous polymer, which is extensively used in flexible packaging. The dual packaging requirements of recyclability and long-term shelf life are often difficult to achieve. Meeting these needs become more urgent when considering food packaging for large volumes of soldiers positioned in different parts of the world. Our approach is to develop a high barrier PET packaging system via the Montmorillonite layered silicate (MLS) based nano technology. Prior research has indicated the significant impact of the polymer crystalline regions on the properties of the resultant nanocomposite. Therefore we must first investigate the amorphous PETG. We must also investigate the influence of increased matrix polarity on dispersion of the PETG by incorporating maleic anhydride (MA) onto the PETG backbone. The influence of the clay concentration and maleation are independently investigated. The glass transition of the as-processed and annealed samples are analyzed using Differential Scanning Calorimetry (DSC) while the thermal stability is determined using Thermogravimetric Analysis (TGA). Testing showed a slight depression in the glass transition temperature of PETG film when the MLS is introduced into the system. The nanocomposite films also demonstrated a lower thermal stability in relation to the neat PETG films. The barrier properties were determined on an in-house built calibration unit based on atomic mobility under high vacuum. X-ray diffraction and TEM were utilized to determine the dispersion of the MLS in PETG. The results indicate that the dispersion was concentration independent but maleation of the PETG led to a slight decrease in agglomeration. An increased ultimate tensile strength and modulus was observed in PETG nanocomposites. The barrier properties were improved by incorporating the MLS into the system. Maleation of the PETG resulted in significant yellowing of the nanocomposites.

Introduction

Polymer/MLS nanocomposites have found numerous applications in various fields. There has been extensive interest in the development of polymer layered-silicate nanocomposites. Improved barrier properties, higher mechanical strength, improved flame retardance, and increased dimensional stability have been observed in polymer nanocomposites. These properties were obtained without significantly raising the density of the compound or reducing light transmission [3-5].

To make a successful nanocomposite, it is very important to be able to disperse the inorganic material throughout the polymer. If a uniform dispersion is not achieved, agglomerates of inorganic material are found within the host polymer matrix, thus limiting improvement. In particular, barrier properties are associated with existence of the tortuous path therefore; an exfoliation or separated layer configuration is vital to architecturally engineering high barrier materials [6].

Factors limiting successful dispersion of the layered silicates are the hydrophilic nature of the silicates and the largely hydrophobic nature of most engineering polymers. To produce an intercalated nanocomposite, the polymer has to wet the clay particles to some extent so that the polymer chains are intercalated between the MLS galleries. To make delaminated or exfoliated nanocomposites, a higher degree of wetting is required. To enhance polymer-clay interaction, the MLS interlayer surfaces of the silicate are chemically treated to make the silicate less hydrophilic and therefore more wettable by the polymer [7-10].

Polyethylene terephthalate glycol (PETG) described generally as polyethylene 1,4 cyclohexylenedimethylene terephthalate is an amorphous thermoplastic of the PET family. PETG has excellent clarity, good impact and tear strength at low temperatures, and excellent resistance to stress and bend whitening. PETG has excellent gas barrier properties, which makes it an outstanding choice for storing biologicals. Presence of 1,4 cyclohexane dimethanol keeps PETG from crystallizing. The presence of bulky 1,4 cyclohexane dimethanol group in the main chain unit makes PETG highly amorphous with no crystalline melting point [1,2].

Experimental

Materials

An extrusion grade of amorphous copolyester resin (Eastar 6763) was supplied in pellet form by Eastman Chemical Company.

Montmorillonite layered silicate (MLS 20A) clay was supplied by Southern Clay Products.

A 99% pure grade of maleic anhydride from Research Chemicals Ltd. was used as a compatibilizer for the polymer and clays. Its purpose was to assist in developing a copolymer in which a more hydrophobic end (PETG) is tied to a more hydrophilic end (MA).

Nanocomposite Preparation

PETG pellets were dried overnight in a vacuum oven at 80°C to remove any moisture from the polymer. The MLS and polymer were compounded on a Thermoprism twin-screw extruder (TSE-16) with co-rotating, completely intermeshing, 16mm screws at a L/D ratio of 24:1. Individual MLS concentrations of (1, 2, 3 & 5%) were prepared by mixing appropriate amounts of the nanocomposite master batch with neat PETG. PETG/maleic anhydride master batch was prepared under the same processing conditions. Individual nanocomposites of 1,2,3, and 5% by weight MLS were prepared from the PETG-MA master batch to create the desired maleated system.

Preparation of Nanocomposite Film

All PETG/MLS nanocomposite pellets were dried overnight in a vacuum oven at 80°C to remove moisture from the polymer. PETG nanocomposite films of 10-mil thickness were extruded into film on a ThermoHaake Polydrive Single Screw Extruder equipped with a slit die. Chilled rolls, set at a temperature of 17.5°C, were used to form the films.

X-ray Diffraction (XRD)

XRD experiments were carried out on a Siemens D500 x-ray diffractometer. The experiments were carried out at room temperature with a scanning speed of 1°/min and a step

size of 0.02 μ m. Experiments were carried out on a powdered sample of PETG/MLS nanocomposites. The basal spacing (d spacing) was calculated by using Bragg's equation.

Differential Scanning Calorimetry (DSC)

DSC scans were run on a Thermal Analysis (TA) Q100 series DSC. Two controlled heat/cool cycles were used in order to analyze the samples. Scans were conducted from a temperature of 15°C to 270°C at a rate of 10°C/min.

Transmission Electron Microscopy (TEM)

The TEM study was conducted on a JEOL JEM-100CX II electron microscope.

Mechanical Properties

An MTS 810 hydraulic system was used for tensile testing of PETG nanocomposite films. ASTM standard (D882-95a) was used to measure tensile properties of thin PETG films.

Permeability

Helium permeability experiments were performed on a house built permeability instrument. The principle of the instrument is based on measuring the rate of diffusion of a penetrant gas molecule in a closed high seal system. All the experiments were carried out on 10-mil thick PETG films. Helium was used as an experimental gas.

Results and Discussion

The dispersion of layered silicates within the PETG and maleated PETG was examined by x-ray diffraction. The organophilically treated clay Cloisite-20 A has two characteristic peaks at low 2 θ equal to 4.4 $^\circ$ (001) and 8.9 $^\circ$ (002). The peak (001) corresponds to an average basal spacing of 19.8 Å and the peak (002) has a basal spacing of 9.9 Å . Figures 1 & 2 show the x-ray diffraction pattern of PETG/Cloisite-20A nanocomposites with and without maleic anhydride. All the nanocomposites showed a shift to lower 2 θ values compared to that of the Cloisite-20A characteristic 001 peak position.

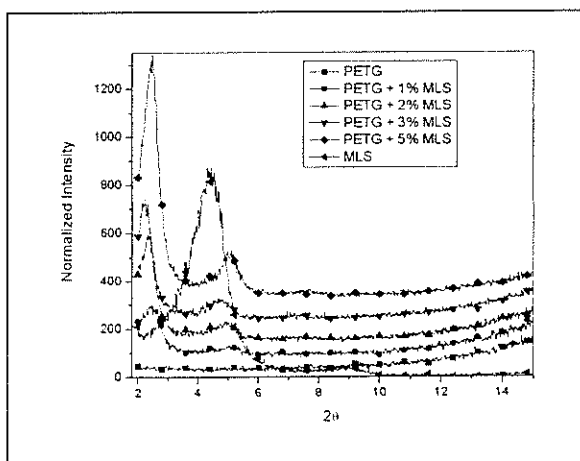


Figure1. XRD of PETG nanocomposites

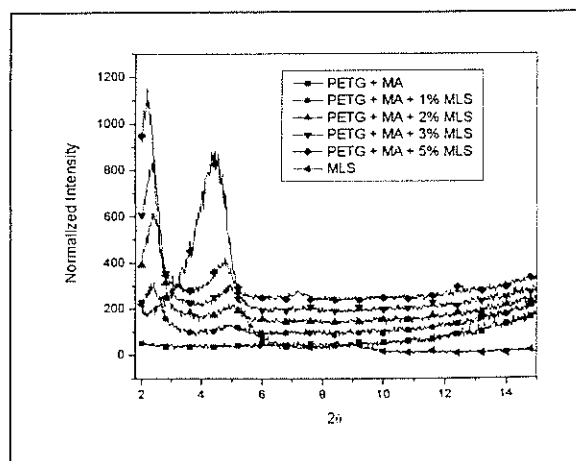


Figure2. XRD of MA+PETG nanocomposites

These results indicate an intercalated dispersion. TEM micrographs of 1% nanocomposites with and without maleic anhydride are shown in Figures 3 & 4 respectively. The

platelet spacing was analyzed using NIH-Image. Table 1 shows the platelet spacing observed in x-ray diffraction and Transmission Electron Microscopy (TEM). No concentration effect of clay was observed on the peak position but intensity increased with concentration. The basal spacings observed in x-ray diffraction matched the one observed in TEM.



Figure3. TEM, 1% PETG nanocomposites.

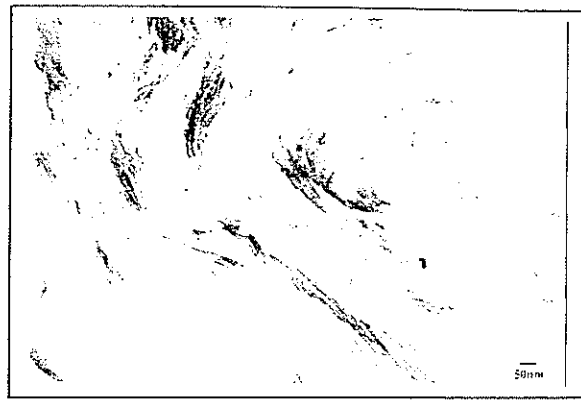


Figure4. TEM, 1% PETG+MA nanocomposites.

Table1. TEM platelet spacing

	PETG Nanocomposites		PETG - MA nanocomposites	
	X-ray	TEM	X-ray	TEM
Clay	19 Å ^o	-	19 Å ^o	-
1%	35 Å ^o	30 Å ^o	37 Å ^o	40 Å ^o
2%	37 Å ^o	35 Å ^o	37 Å ^o	35 Å ^o
3%	39 Å ^o	36 Å ^o	37 Å ^o	38 Å ^o
5%	35 Å ^o	35 Å ^o	39 Å ^o	35 Å ^o

Table2. FWHM, PETG Nanocomposites

Name	Peak (001) FWHM	Peak (002) FWHM
Cloisite 20A	1.1	1.02
1% MLS	.43	.75
2% MLS	.30	.69
3% MLS	.30	.69
5% MLS	.35	.54

Tables 2 & 3 show the full width half maxima (FWHM) of 001 and 002 peaks. The peaks became narrower with increasing clay concentration. This is an indication of a strong intercalated behavior. Vaia has also reported similar results in nylon nanocomposites. The decreased FWHM behind this strong effect is attributed to strong platelet-to-platelet interaction [11].

Maleated nanocomposites show larger FWHM values compared to nanocomposites without maleic anhydride. This indicates more structural disorder due to presence of MA as a compatibilizer. Low molecular weight MA acted as a coupling agent and a better dispersion was observed.

Table3. FWHM PETG-MA Nanocomposites.

Name	Peak (001) FWHM	Peak (002) FWHM
Cloisite 20A	1.1	1.02
MA+1% MLS	.46	.83
MA+2% MLS	.41	.69
MA+ 3% MLS	.34	.68
MA+ 5% MLS	.30	.58

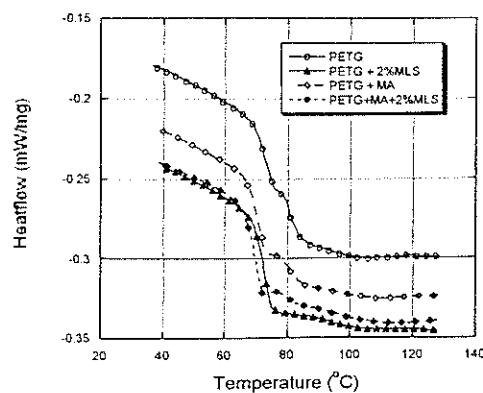


Figure 5 shows the effect of MLS on the glass transition of PETG. A decreasing trend of glass transition temperature was observed in PETG nanocomposites. T_g of PETG and PETG with maleic anhydride were similar indicating no plasticizing of the PETG chains due to low molecular weight maleic anhydride. All nanocomposite samples showed plasticization of the polymer due to the MLS. It is likely that the chains do not pack tightly on the silicate surface and are therefore more mobile. Further since there is an intercalated dispersion, which is concentration independent, it is likely that a fixed fraction of chains is trapped between the platelets and therefore there are significant unconstrained polymer chains in each nanocomposite, which increases with MLS concentration.

Table4. Mechanical PETG Nanocomposites.

Type	UTS, Mpa	Strain to Failure	Modulus, GPa
PETG	53	.049	1.2
PETG + 1%MLS	55	.048	1.2
PETG + 2%MLS	56	.044	1.2
PETG + 3%MLS	56	.041	1.3
PETG + 5%MLS	58	.041	1.4

Table5. Tensile PETG-MA Nanocomposites.

Type	UTS, Mpa	Strain to Failure	Modulus, GPa
PETG+MA	46	.052	1.0
PETG+MA+1% MLS	47	.041	1.3
PETG+MA+2% MLS	50	.040	1.3
PETG+MA+3% MLS	48	.034	1.3
PETG+MA+5% MLS	49	.035	1.2

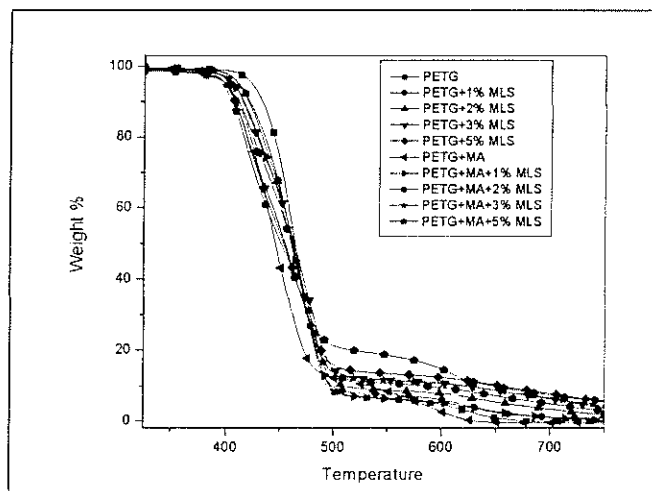


Figure6. Thermal behavior of PETG Nanocomposites.

TGA was performed on Closite-20A to study the decomposition behavior. Closite-20A has a decomposition temperature of 305°C. PETG processing was done below 300°C. Previous studies show that a better compatibility between polymer and clay can be achieved between clay and polymer by using a modifier that is stable at polymer processing temperature.

Tables 4 & 5 show the mechanical properties of PETG nanocomposites. Nanocomposites without maleic anhydride showed a maximum 10% increase in UTS and 16% increase in

modulus. Low molecular weight maleic anhydride played a dominant role and a 5% decrease in UTS was observed in maleic anhydride clay nanocomposites compared to neat PETG.

Figure 6 shows the degradation behavior of PETG nanocomposites. All PETG nanocomposites showed a 3-5% drop in the degradation temperature. The MLS have been treated with an organic modifier. The initial weight loss in the TGA studies corresponds to degradation of this organic treatment. The degradation onset temperature dropped from 426°C to 400°C, which is well above the working temperature of PETG. While the surfactant degradation was not accompanied by any significant weight loss, it is apparent that the degraded surfactant reacted and accelerated the degradation of the PETG.

PETG nanocomposites showed improved resistance towards helium gas. No concentration dependent effect was observed and the 1% MLS loading sample showed the best results.

Conclusion

Maleic anhydride served as an effective compatibilizer but the un-reacted maleic anhydride contributed to decreased thermal stability due to the reactivity with the hydrogenated tallow. Intercalated dispersion was observed in x-ray diffraction and TEM confirmed the platelet spacing observed in the x-ray diffraction patterns. Non-maleated nanocomposites showed a 10% increase in UTS and 16% increase in modulus. Maleation of PETG resulted in a permanent set of the polymer similar to maleated polypropylene but the ductility came at the cost of rigidity. When MLS was added, the rigidity was regained but ductility decreased. It is evident therefore that the maleated PP benefits are concomitant to the heterogeneous nucleation promoted by MLS. Therefore our current work is directed towards semi crystalline PET. Barrier properties towards helium gas were found to improve. A slight decrease in degradation temperature of nanocomposites was observed. Addition of MLS showed a decrease in glass transition temperature. Stiff platelets with intercalated dispersions resulted in decreased chain packing and increased free volume. These affects are believed to contribute to a decreased T_g .

Acknowledgement

The authors would like to thank Teresa Golden for use of her XRD facilities and David Garrett for microscopy assistance at UNT. This work could not have been accomplished if not for the Strategic Environmental Research and Development Program (SERDP) and Southern Clay Products.

References

1. Brydson J., *Plastics materials*, Butterworth Heinemann 1999.
2. Saunders K.J., *Organic Polymer Chemistry*, Chapman and Hall 1988.
3. Kojima Y, Fukumori K, Usuki A, Okada A, Kurauchi T. *J. Mater Sci Lett*, 1993;12:889.
4. Giannelis E.P. *Adv mater*, 1996, 8:1:29.
5. Krishnamoorti R, Vaia R.A, Giannelis E.P, *Chem Mater*, 1996, 8:1728.
6. Pinnavaia T.J., Beall G.W., *Polymer Clay nanocomposites*, 2001.
7. Bidadi H, Schroeder PA and Pinnavaia TJ, *J. Phys. Chem. Solids* 1998, 49:12: 1435.
8. Burnside SD and Giannelis EP, *Chem. Mater.* 1995, 7:9: 1597.
9. T. Lan and T.J. Pinnavaia, *Chem. Mater.*, 1994, 6:12:2216.
10. X. Kornmann, L.A. Berglund and J. Sterte, *Polymer Eng. & Sci.*, 1998, 38:8:1351.
11. Vaia R., Giannelis P., *Macromolecules* 1997, 30:8000.